

## RESEARCH ARTICLE

# Priority Selection of Road Traffic Net-Works in Emergency Situations Based on Internet of Vehicles

XILIANG WANG AND HUIJIAN GENG<sup>1b</sup>

School of Traffic and Transportation, Shijiazhuang Tiedao University, Shijiazhuang 050043, China

Corresponding author: Huijian Geng (zhangjessie19@sina.com)

**ABSTRACT** The current emergency vehicle priority control methods in road traffic net-works are difficult to cope with the increasing traffic demand. Therefore, a traffic control method based on multi-vehicle collaborative lane change strategy, fleet convergence and gap adjustment model is proposed and its effectiveness is verified. These experiments confirmed that the speed of vehicle  $C_{j+1}$  under strategy 1 showed a positive correlation with time at 0-5s, reaching an extreme value of 16.85 m/s around 4s, and a negative correlation after 5s. Under strategy 2, its speed showed a negative correlation with time at 0-4s, and a parallel relationship after 4s. The multi-vehicle collaborative lane changing strategy was validated. Except for fleet C with a density of  $+0.0333m^{-1}$ , the actual adjustment time of vehicle C1 was gradually increasing at all other densities. The maximum time for B1 adjustment was 9.358s, and the maximum time for C1 adjustment was 10.798s. The longitudinal relative displacement of C1 was larger than that of B1. In addition, compared with Model T, the research method increased the average vehicle speed by 12.64% under four different flow rates. Compared with Model Y, the average flow rate of the research method under the four experimental flows was 1.45%. Overall, the research method is effective and feasible in the priority selection control of road traffic net-works. It improves the operational efficiency of emergency vehicle sections and can be effectively applied in actual traffic net-works.

**INDEX TERMS** Vehicle networking, emergency situations, multi-vehicle collaborative lane changing strategy, IAWM, traffic volume.

## I. INTRODUCTION

The number of abnormal deaths caused by emergencies is increasing every year, which has brought huge losses to the lives and property of people, and the situation of public safety is very severe [1], [2], [3]. With the continuous deepening of urbanization, population and resources continue to be concentrated in urban areas. The growing aging population has also led to a sharp increase in urban emergency needs in emergency situations [4], [5]. Emergency Vehicles (EVs) are important carriers for responding to urgent needs. Reducing their actual response time has become a major goal in developing emergency rescue systems [6], [7], [8]. Only when emergency rescue personnel arrive at the

scene in a timely manner can the success rate of rescue be improved and the lives and property of people be maximally re-stored. However, the sharp increase in car ownership has led to increasing congestion in urban road net-works, which reduces the ability of EVs to quickly reach emergency sites. In addition, the accident rate of EVs is also showing a growing trend [9]. Therefore, an urgent issue that needs to be addressed is to study the priority traffic control methods for EVs in urban road net-works, improve their efficiency, reliability, and safety, and reduce their adverse effects on daily traffic [10], [11]. Some scholars have conducted research on vehicle lane changing and proposed dynamic lane changing models in the context of mixed traffic. When changing lanes, considering both human driver behavior and fleet spacing has certain limitations [12]. There are multiple options in the current priority control methods for emergency vehicles.

The associate editor coordinating the review of this manuscript and approving it for publication was Wei Quan.

For example, by developing an intelligent alarm system for ambulances, reminding the surrounding social vehicles to give way. By designing an emergency vehicle detection system, supported by sensing technology, a low-density road for emergency vehicles was found to pass through. Alternatively, in the context of connected vehicles, considering the efficiency of real-time information exchange between vehicles, a pre-clearing strategy for emergency lanes was designed. In this case, the lane changing model in the priority selection control of traditional road traffic net-works only considers its own speed and the fleet gap of the target lane. It has not been studied from the perspective of Multi-vehicle Collaborative Lane Changing (MVCLC), resulting in low lane changing efficiency. And it lacks research on fleet automatic yielding, which leads to low driving efficiency of EVs. Therefore, the study utilizes the MVCLC strategy to construct a fleet flow and gap adjustment model, and proposes the Internet of Vehicles-Based Automatic Way Giving Method (IAWM) for emergency situations. The research aims to improve the lane changing efficiency of vehicles in emergency situations from the perspective of multi-vehicle collaborative lane changing, in order to improve the driving efficiency of emergency vehicles and enrich the research content of vehicle networking technology in this field.

In response to the shortcomings of current emergency vehicle priority control methods, research is conducted from the perspective of multi-vehicle cooperation for lane changing, taking into account various factors such as road traffic density and initial vehicle status. Multiple models such as fleet gap adjustment are constructed. Mean-while, corresponding fleet automatic yield control methods are proposed. Problems such as the relative position relationship of vehicles in the fleet and the minimum distance of the fleet during lane changing are solved in this study. Overall, the research methodology is more comprehensive and helps to improve lane changing efficiency.

The total research is divided into four parts. The first part is to summarize and discuss the current approaches about emergency vehicle preference control in road traffic net-works. The second part is to analyze the proposed multi-vehicle cooperative lane-changing strategy, convoy convergence and gap regulation model, and the final IAWM method using Telematics. The third part is the validation of the IAWM method and the fourth part summarizes the whole article.

## II. RELATED WORKS

When passing on road sections, EVs mainly rely on emergency avoidance by vehicles ahead to ensure rapid passage. Due to the lack of effective communication technology in the past, research in this field is relatively scarce. With the development of IoV, fast communication between vehicles is achieved, which has aroused the research interest of scholars [13], [14]. Liu Z et al. aimed to improve the driving efficiency of EVs under high road traffic density, and an automatic yielding system was designed by utilizing

vehicle to vehicle communication in IoV. This effectively improved the operating efficiency of EVs and enhanced their automatic avoidance performance while considering traffic density [15]. Cao M et al. proposed an emergency IoV priority selection control method using greedy mechanism and deep reinforcement learning to address the issue of rapid response of EVs in emergency situations. This effectively reduced traffic conflicts and negative impacts, and improved the driving efficiency of EVs [16]. Hosseinzadeh et al. proposed a new traffic control scheme for EV in traffic congestion by utilizing centralized computing technology and IoV, which not only improved the driving efficiency of EV but also helped to quickly disperse vehicles in congested sections [17]. Alkhatib A et al. proposed an intelligent urban road traffic control management system for the intelligent EVs scheduling in congested urban road net-works, taking into account urban traffic flow. This effectively reduced the actual running time of EVs [18].

In addition, Raja G et al. proposed a multi-agent deep reinforcement path optimization algorithm for emergency rescue vehicles, utilizing 6G net-works and autonomous IoVs. This algorithm effectively reduced travel time while improving the efficiency of EV operation and provided assistance in enhancing rescue efficiency [19]. Antonio and Maria-Dolores proposed a traffic control method based on 5G communication and IoV to address the priority traffic control of EVs in urban transportation net-works, effectively reducing the travel and congestion time of EVs [20]. Jutury et al. proposed an intelligent EV priority control method based on neural fuzzy to effectively improve the driving efficiency of EVs due to the exacerbation of traffic congestion speed, which led to lower actual operating efficiency [21]. Hajiloo et al. proposed an integrated vehicle effective traffic control method based on IoV for the comprehensive traffic control problem of vehicles in emergency situations, thereby effectively improving the rescue efficiency of EVs [22].

Based on the above research, the current EV priority traffic control method in the road traffic net-work is difficult to cope with the increasing traffic demand. However, traditional lane changing models only consider their own speed and the fleet gap of the target lane, without considering MVCLC. Therefore, the IAWM proposed from the perspective of MVCLC strategy is innovative. In theory, innovative research has proposed MVCLC strategies, fleet convergence, and gap adjustment models in the IoV environment, effectively improving the EV priority traffic theory in IoV. In practice, the proposed method provides an important theoretical basis for improving the driving efficiency of EVs in practice, and helps managers implement EV rescue scheduling. Research on collaborative lane changing strategies and priority communication control methods for emergency vehicle sections is beneficial to promoting the improvement of lane changing efficiency to a certain extent. Studying the addition of fleet automatic yield control methods can be helpful in solving the problem of low driving efficiency of emergency vehicles.

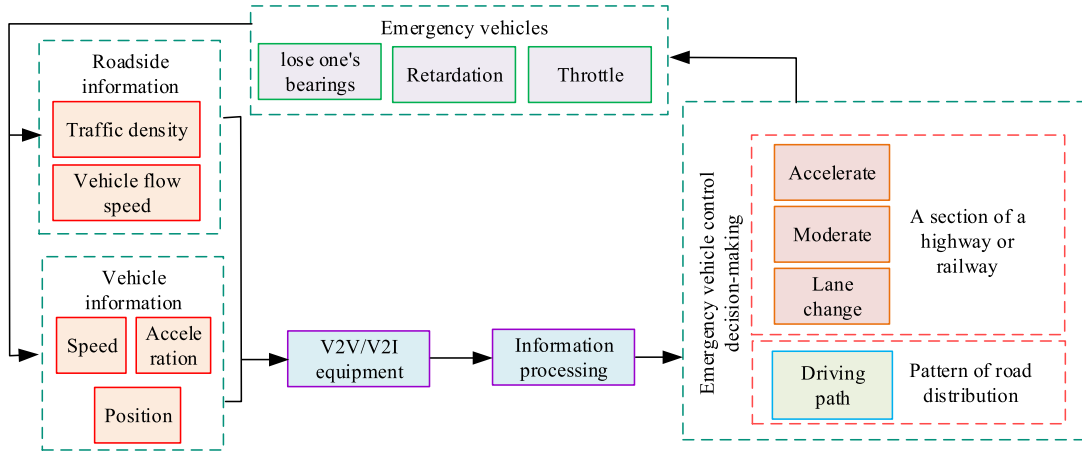


FIGURE 1. Decision-making process.

### III. THE PRIORITY SELECTION PROBLEM OF EMERGENCY VEHICLE TRAFFIC NET-WORK BASED ON THE INTERNET OF VEHICLES

Under the traditional management mode of emergency vehicle traffic, social vehicles are unable to complete lane changes in a short period of time and make way for EVs in a timely manner. This seriously affects the efficiency of emergency vehicle traffic. Therefore, this section mainly analyzes the MVCLC strategy, fleet convergence and gap adjustment model, and the proposed IAWM.

#### A. MULTI-VEHICLE COL-LABORATIVE LANE CHANGING STRATEGY UTILIZING CONNECTED VEHICLES IN EMERGENCY SITUATIONS

This study proposes an IAWM to address the issue of EV priority traffic control methods being un-able to cope with the growing traffic demand environment in the current road traffic net-work. The current development of information technology is driving the expansion of IoV, enabling real-time communication between vehicles. Real-time communication between different vehicles can timely inform the drivers of other vehicles of the driving situation of EVs, and further improve the maneuverability and safety of EVs. Firstly, the decision-making process of emergency vehicle driving is analyzed in the context of connected vehicles, as shown in Figure 1.

In Figure 1, the driving path of EVs is determined based on the operational status of the road net-work at the road net-work level. The ac-celeration, de-celeration, lane changing, and overtaking behaviors of EVs are determined within the road section based on traffic density and the driving status of surrounding vehicles. Under normal circumstances, EVs will choose the inner lane when driving on real roads. However, vehicles on the inner lane will turn to adjacent lanes after receiving commands, and there are rarely cases of entering the outer vehicle lane from adjacent lanes [23], [24], [25]. Therefore, the study aims to focus on the complexity of the model and select a two-way two-lane high-way as the

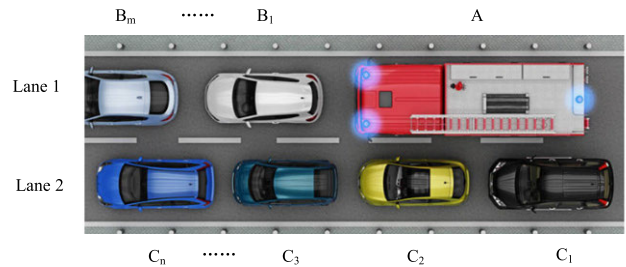
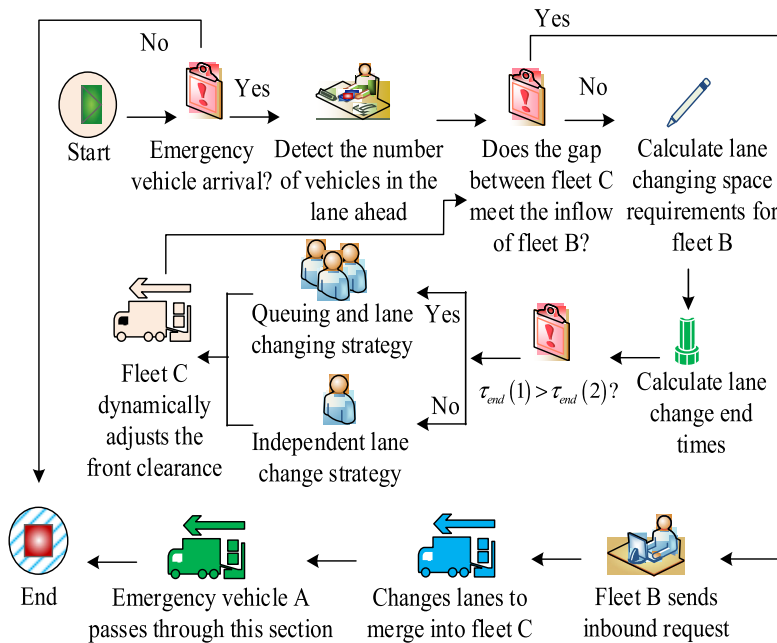


FIGURE 2. Schematic diagram of simulated scenarios for intelligent yielding of emergency vehicles in actual operation.

research object to analyze the entire process of vehicles automatically giving way in emergency situations. This process does not consider the impact of pedestrian crossing, signal control and other factors on vehicle queues. Figure 2 shows the specific simulation scenario.

From Figure 2, it is assumed that the fleet on lane 1 with EV is the original fleet, i.e. fleet B, while the fleet on lane 2 without EV is the target fleet, i.e. fleet C. Therefore, based on the driver’s habit of overtaking on the left during actual traffic, lane 2 is defined as the lane of passage of EV. After receiving the passage message from the relevant EV in fleet B, all vehicles immediately find a suitable location in fleet C, judge whether to add or subtract, and issue a transfer request to the corresponding vehicles in fleet C. The vehicles of fleet C adjust their speed and interval according to this requirement to meet the need for lane changing and merging within fleet C. After the interval adjustment is completed, a message is sent to fleet C’s vehicles to enter. Figure 3 shows the specific operation process.

From Figure 3, the process first determines whether EVs have reached. If not, the process ends. If so, the specific number of vehicles inside the lane ahead is detected. Secondly, it is determined whether the gap between fleet C met the merging requirements of fleet B. If so, fleet B sends relevant merging requests and merges them into fleet C. At this point, EV A



**FIGURE 3. Control process flowchart of intelligent yielding of emergency vehicles in actual operation.**

can pass through the section of the road and end the process. If not, it is necessary to calculate the lane changing space requirement of fleet B and the end time of lane changing for vehicles 1 and 2. If the former is greater than the latter, a queue lane changing strategy is executed. If not, an independent lane changing strategy is executed. Then, fleet C dynamically adjusts the gap at the front of the vehicle and re-judges whether the gap meets the merging of fleet B. Finally, the process ends.

Normally, when there are vehicles present in two lanes, the traffic flow on the road is already quite dense. Therefore, it takes a long time to achieve the convergence of two teams of vehicles. The study intends to use the minimum time to design a flow control method that allows the two teams of vehicles to quickly adjust their speed and position in the shortest possible time. All vehicle dynamics are set to be equal. To simplify practical modeling, and the longitudinal vehicle control is emphasized without considering lateral vehicle control. The actual position of vehicles in fleet B is projected onto fleet C to create a virtual channel and merge the fleet. In this process, effectively analyzing the distribution probability of actual lane changing gaps for vehicles is the key to proposing a multi-vehicle system lane changing strategy. According to the basic principle of traffic flow, it is necessary to determine whether the number of vehicles arriving at a certain moment or the number of vehicles allocated at a certain distance satisfies a Poisson distribution. Its basic expression and the probability distribution of the distance between the front of the vehicle are represented by equation (1) [26], [27], [28].

$$\begin{cases} X(\kappa) = \frac{(\psi\tau)^\kappa e^{-\psi\tau}}{\kappa!} \\ E(p) = X(0) = e^{-\psi(p/v)} = e^{-\kappa p} \end{cases} \quad (1)$$

In equation (1),  $X(\kappa)$  represents the probability of  $\kappa$  vehicles arriving with a counting time interval of  $\tau$ .  $\psi$  represents the actual achievement rate of the vehicle.  $E(p)$  represents the probability of the distribution of head-way within a unit length of  $p$ .  $v$  represents the actual speed of the vehicle. From equation (1), the vehicle time distance on a single-lane at a given moment exhibits a negative exponential distribution. Then, it is assumed that the positional relationship between vehicles in the simulation scenario is a same direction intersection in different lanes. Vehicles in lane 1 can merge into lane 2 at any time, but their tails are exactly parallel to the front of vehicles in lane 2. Therefore, in this case, vehicles in lane 2 need to consider safety issues and adjust the distance between their heads (this analysis process does not consider vehicles behind). It is assumed that vehicles  $B_j$  and  $B_{j+1}$  in lane 1,  $C_j$  and  $C_{j+1}$  in lane 2, the initial position of the rear EV's front end is  $X_0$ , the initial positions of the front end of  $B_j$  and  $B_{j+1}$  are  $X_{C0}$  and  $X'_{C0}$ , and the initial positions of the front end of  $C_j$  and  $C_{j+1}$  are  $X_{B0}$  and  $X'_{B0}$ . When the counting time interval  $\tau$  is within  $[0, \tau_v]$ , the relevant distance relationship satisfied by vehicle  $C_j$  is represented by equation (2).

$$\begin{cases} J_{AB0} + \int_{\tau_0}^{\tau_v} v_B(\tau) d\tau = J_{AC0} + \int_{\tau_0}^{\tau_v} v_C(\tau) d\tau + J_{CB} \\ v_C(\tau_v) = v_B(\tau_v) \\ J_{CB} = h_v + J_{Q\min} \end{cases} \quad (2)$$

In equation (2),  $J_{AB0}$  is the initial spatial distance between vehicle  $B_j$  and EV A.  $\tau_v$  represents the time point when all vehicles meet the safety lane changing conditions.  $v_B$  means the actual driving speed of vehicle  $B_j$ .  $J_{AC0}$  refers to the

initial spatial distance between vehicle Cj and EV A.  $v_C$  is the actual driving speed of vehicle Cj.  $J_{CB}$  refers to the actual spatial distance between vehicle Cj and Bj.  $h_v$  represents the actual vehicle length.  $J_{Q\min}$  means the minimum safe distance between two vehicles. The relevant distance satisfied by vehicle Cj+1 is represented by equation (3).

$$\begin{cases} J_{AB0} + \int_{\tau_0}^{\tau_v} v_B(\tau) d\tau = J'_{AC0} + \int_{\tau_0}^{\tau_v} v'_C(\tau) d\tau + J'_{CB} \\ v'_C(\tau_v) = v_B(\tau_v) \\ J_{AC} + \int_{\tau_0}^{\tau_v} v_C(\tau) d\tau + (h_v + J_{Q\min}) \\ \leq J'_{AC0} + \int_{\tau_0}^{\tau_v} v'_C(\tau) d\tau \end{cases} \quad (3)$$

In equation (3),  $v'_C$  refers to the actual driving speed of vehicle Bj+1.  $J'_{CB}$  means the actual spatial distance between vehicles Bj and Cj+1.  $J'_{AC0}$  is the initial spatial distance between vehicle Bj+1 and EV A. The relevant distance satisfied by vehicle Bj+1 is represented by equation (4).

$$\begin{cases} J_{AB0} + \int_{\tau_0}^{\tau_v} v_B(\tau) d\tau = J'_{AB0} + \int_{\tau_0}^{\tau_v} v'_B(\tau) d\tau - J_{BB} \\ v'_B(\tau_v) = v'_C(\tau_v) \\ J_{AB0} + \int_{\tau_0}^{\tau_v} v_C(\tau) d\tau + (h_v + J_{Q\min}) \\ \leq J'_{AB0} + \int_{\tau_0}^{\tau_v} v'_B(\tau) d\tau \end{cases} \quad (4)$$

In equation (4),  $v'_B$  represents the actual driving speed of vehicle Bj+1.  $J_{BB}$  represents the actual spatial distance between vehicles Bj and Bj+1. When the counting time interval  $\tau$  is within  $(\tau_v, \tau_{end}]$ , vehicles Bj and Bj+1 will change to lane 2. At this time, the relative distance between EV and vehicle Bj is represented by equation (5).

$$\begin{cases} J_{AB0} + \int_{\tau_0}^{\tau_{end}} v_B(\tau) d\tau = \int_{\tau_0}^{\tau_{end}} v_A(\tau) d\tau - J_{AB} \\ J_{AB} = h_v + J_{Q\min} \end{cases} \quad (5)$$

In equation (5),  $v_A$  represents the actual driving speed of EV A.  $J_{AB}$  represents the spatial distance between vehicle Bj and EV A. Supported by equations (2) to (5), for the MVCLC in the simulation scenario, the in-dependent and queuing lane changing processes in Figure 3 will appear, with strategies implemented in both processes set to 1 and 2, respectively. Therefore, in strategy 1, the spatial distance between vehicle Cj, Cj+1, and Bj is first adjusted. Secondly, the vehicle Bj+1 adjusts its actual speed and spatial distance according to the actual positions of Bj and Cj+1. Therefore, the relative safe distances of vehicles Bj, Bj+1, and Cj+1 at this time are represented by equation (6).

$$\begin{cases} J'_{BC} = h_v + J_{Q\min} \\ J_{BB} = 2(h_v + J_{Q\min}) \end{cases} \quad (6)$$

In strategy 2, the relative distance between vehicles Bj and Bj+1 is first measured, and then vehicle Cj adjusts its actual speed and spatial distance based on their positions. Therefore, in strategy 2, the relative safe distance between vehicles Bj, Bj+1, and Cj+1 is represented by equation (7).

$$\begin{cases} J'_{BC} = 2(h_v + J_{Q\min}) \\ J_{BB} = h_v + J_{Q\min} \end{cases} \quad (7)$$

Through the design of two different strategies, MVCLC is sufficient to respond to different emergency situations before giving way to EVs.

### B. INTELLIGENT YIELD CONTROL METHOD FOR FLEET USING VEHICLE NET-WORKING

On the basis of the MVCLC strategy, the study proposes IAWM, which includes constructing a target fleet gap dynamic adjustment model, an original fleet dynamic convergence model, and calculating the minimum communication distance [29]. The overall process of the IAWM method is shown in Figure 4.

In Figure 4, first, an analysis of the lane changing space requirements for Team B is conducted. In the analysis of lane changing space requirements for fleet B under the dynamic adjustment model of target fleet gap, it is assumed that there is a cross relationship between the initial positions of these two lane fleet. The initial position of EV A in lane 1 is  $X_{A(\tau_0)}$ , the nearest vehicle in front of it is B1, and the spatial distance between them is  $J_{AB1(\tau_0)}$ . The initial position of the vehicle is  $X_{B1(\tau_0)}$ , while the initial position of vehicle C1 in lane 2 is  $X_{C1(\tau_0)}$ . Therefore, according to the relevant definition of traffic density, the actual center distance between adjacent vehicles in the actual initial state is represented by equation (8) [30], [31].

$$\begin{cases} J_{B0} = \frac{1}{\kappa_B} \\ J_{C0} = \frac{1}{\kappa_C} \end{cases} \quad (8)$$

In equation (8),  $J_{B0}$  and  $J_{C0}$  represent the center distance between adjacent vehicles in lanes 1 and 2, respectively.  $\kappa_B$  and  $\kappa_C$  mean the densities of fleet B and C, respectively. Under the relevant traffic requirements of the EV, the preceding vehicles adjust their intervals and change lanes according to the unit number sequence. After the lane change control moment is activated, the first car Cn in fleet C will be limited by the speed of the preceding vehicle and the road surface and will move forward at speed  $v_C$ . Other vehicles in fleet C need to adjust their speed. When two adjacent vehicles in fleet C can be used for vehicle merging, the existing gap is  $P_{A0} = 1/\kappa_C - (J_v + J_{Q\min})$ , ensuring that all vehicles in fleet B can safely merge into fleet C. When the minimum additional gap between adjacent vehicles in fleet C is  $P_{Cj} = (J_v + J_{Q\min}) - P_{C0} = 2(J_v + J_{Q\min}) - 1/\kappa_C$ , the actual minimum additional gap required for all vehicles in fleet B to merge into fleet C is represented by equation (9).

$$P_{C1}(\tau_{Bend}) = m(2(J_v + J_{Q\min}) - (1/\kappa_C)) \quad (9)$$

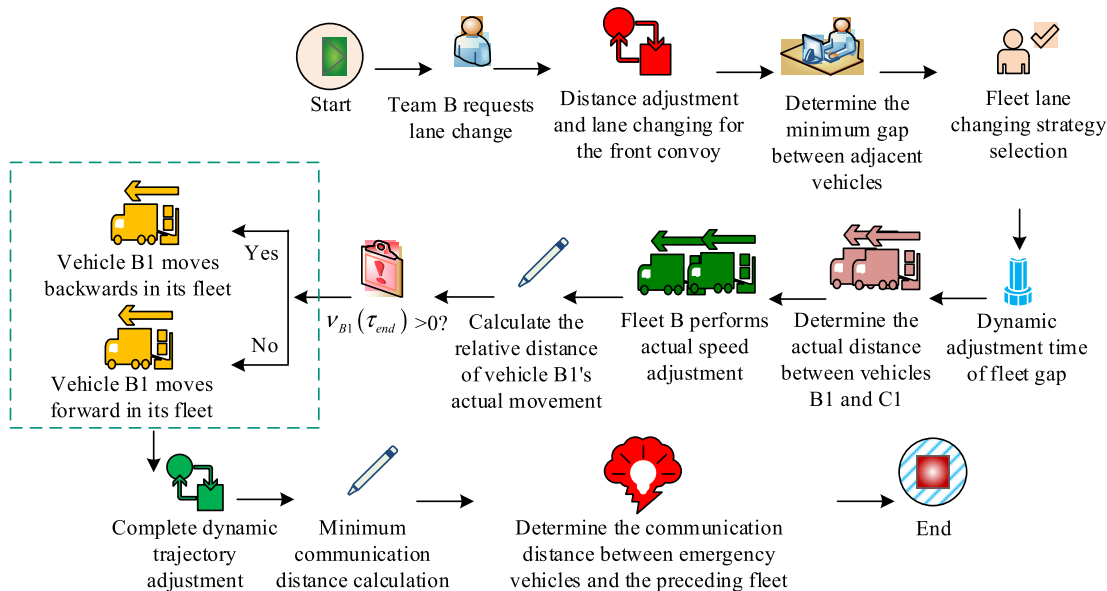


FIGURE 4. The overall process of IAWM method.

In equation (9),  $P_{C1}(\tau_{Cend})$  is the additional gap between vehicles  $C1$  and  $C_{m+1}$ .  $m$  means the number of vehicles in fleet  $C$ . Because the actual driving speed of vehicle  $C_{m+1}$  is  $v_C$ , vehicle  $C1$  achieves  $P_{C1}(\tau_{Cend})$  through de-acceleration, represented by equation (10).

$$\begin{cases} P_{C1}(\tau_{Cend}) = \int_{\tau_0}^{\tau_{Cend}} (v_{C0} - v_{C1}(\tau)) d\tau \\ v_{C1}(\tau) = v_C + \int z_{C1}(\tau) d\tau \\ P_{C1}(\tau_{Cend}) = \int_0^{\tau_{Cend}} -z_{C1}(\tau) d\tau \end{cases} \quad (10)$$

In equation (10),  $\tau_{Cend}$  represents the time after the actual speed adjustment of vehicle  $C1$  has ended.  $v_{C1}(\tau)$  means the actual instantaneous speed of vehicle  $C1$  at time  $\tau$ .  $z_{C1}(\tau)$  is the actual acceleration of vehicle  $C1$ . In the analysis of lane changing strategy selection for the target fleet gap dynamic adjustment model, the optimal col-laborative lane changing strategy is designed based on the designed strategies 1 and 2 in Figure 5.

From Figure 5, the actual process of selecting the optimal strategy for col-laborative lane changing among multiple vehicles is first to divide the two fleets into  $m/2$  units. When  $j=1$ , the initial positions of vehicle  $C_{j+1}$  and  $B_{j+1}$  are inputted. If the former is greater than the latter, strategy 1 is implemented. If the former is equal to the latter, strategy 2 is implemented. If the former is less than the latter, these two strategies are combined and implemented according to the actual situation. Secondly, the actual spatial adjustment strategy for fleet  $C$  is determined and  $j$  is added by 1. If the updated  $j \leq m/2$ , the initial positions of vehicle  $C_{j+1}$  and  $B_{j+1}$  will be out-putted again and the process will be repeated. If  $j > m/2$ , the next step will be taken. Finally, the process ends. In the analysis of the actual gap dynamic adjustment

time in the fleet, the equation for the minimum additional gap between adjacent vehicles in fleet  $C$ , the formula in the third row of equation (10), and related equations are combined to calculate the actual speed adjustment time of vehicle  $C1$ . This equation is then combined with the formula in the second row of equation (10) to calculate the time after the actual speed adjustment of vehicle  $C1$  is completed and the actual ac-acceleration of vehicle  $C1$ , represented by equation (11).

$$\begin{cases} m(2(J_v + J_{Qmin}) - (1/\kappa_C)) = \int_0^{\tau_{Cend}} -z_{C1}(\tau) d\tau \\ \begin{cases} z_{C1}(\tau) d^2\tau = m/\kappa_C - 2m(h_v + J_{Qmin}) \\ z_{C1}\tau_{Cend} = v_{min} - v_C \end{cases} \end{cases} \quad (11)$$

The first row of equation (11) is used to calculate the actual speed adjustment time of vehicle  $C1$ , while the second and third rows are used to calculate  $\tau_{Cend}$  and  $z_{C1}$ . In the construction of the original fleet dynamic convergence model, vehicle  $B1$  in lane 1 under the control end of fleet  $B$  happens to be located between  $C1$  and  $C2$  in lane 2. At this point, for the safe lane change of vehicle  $B1$ , the actual distance between vehicles  $B1$  and  $C1$  should be equal to the distance  $B1$  moves relative to  $C1$ , represented by equation (12).

$$|X_{B1}(\tau_{Bend}) - X_{C1}(\tau_{Bend})| = h_v + J_{Qmin} \quad (12)$$

In equation (12),  $\tau_{Bend}$  represents the actual end time of vehicle  $B1$  after adjusting its speed, which is also the end time of the entire fleet  $B$ 's speed adjustment. After the actual speed adjustment is completed, the relative distance of vehicle  $B1$ 's

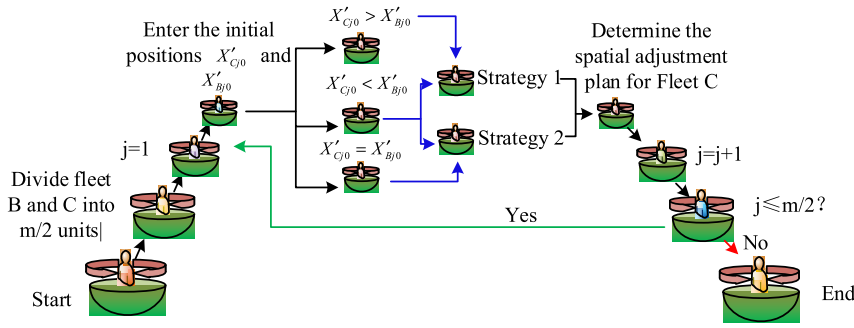


FIGURE 5. Process for selecting the optimal strategy for multi-vehicle col-laborative lane changing.

actual movement is represented by equation (13).

$$\begin{cases} P_{B1(\tau_{Bend})} = P_{Cj} + K_0 - (h_v + J_{Q\min}) \\ = (2m - 1)(h_v + J_{Q\min}) + K_0 - \frac{m}{\kappa_C} \\ P_{B1}(\tau_{Bend}) = \int_0^{\tau_{Bend}} \int_0^{\tau_{Bend}} -z_{B1}(\tau) d\tau \\ (2m - 1)(h_v + J_{Q\min}) + K_0 - \frac{m}{\kappa_C} = \\ \int_0^{\tau_{Bend}} \int_0^{\tau_{Bend}} -z_{B1}(\tau) d\tau \\ v_{B1}(\tau) = v_B + \int z_{B1}(\tau) d\tau \end{cases} \quad (13)$$

In equation (13),  $K_0$  represents the relevant center distance between B1 and C1. The actual relative distance of vehicle B1's movement can be calculated using the first or second row of equation (13), and combining them can obtain the third row of equation (13). The actual speed of vehicle B1 can be calculated using the fourth row of equation (13). If  $v_{B1}(\tau_{end}) > 0$ , the actual relative position of vehicle B1 in its fleet is back-ward. If it is less than 0, it is forward. Based on this, its actual speed may increase or decrease. When using the second line of equation (13), the actual speed of vehicle B1 must be greater than  $v_{\min}$  and lower than the speed limit value, other-wise the actual ac-celeration needs to be adjusted. Therefore, when  $v_{B1}(\tau_{end}) \geq v_{\max}$ ,  $\tau_{Bend}$  is calculated using the equations in the third and fourth rows of equation (13). When  $\tau_{Bend} \leq v_{\min}$ ,  $z_{B1}$  is calculated using the equations in the third and fourth rows of equation (13). The total time required for adjusting the actual dynamic trajectories of fleets B and C is represented by equation (14).

$$\begin{aligned} \tau_{end} &= \max\{\tau_{Bend}, \tau_{Cend}\} \\ &= \max\left\{ \frac{m - \kappa((2m - 1)(h_v + J_{Q\min}) - K_0)}{\kappa(v_{\min} - v_B)}, \frac{m - 2m\kappa(h_v + J_{Q\min})}{\kappa(v_{\min} - v_C)} \right\} \end{aligned} \quad (14)$$

In equation (14),  $\tau_{end}$  represents the total time spent on adjusting the actual dynamic trajectories of fleets B and C. In the analysis of minimum communication distance calculation, after the dynamic orbit adjustment of fleet B and C, all fleet B merges into fleet C. In this situation, the EV happens to reach the rear of the convoy and meets the minimum safe distance  $h_v + J_{Q\min}$  from car B1. Therefore, in emergency

situations, EVs within lane 1 can pass quickly without causing any impact on traffic, greatly improving traffic safety and efficiency. Therefore, the minimum communication distance between EVs and the rear vehicle B1 of the preceding fleet should be greater than  $P_0$  to not affect the rapid passage of EVs.  $P_0$  represents the distance between vehicle B1 and EVs in the initial state, represented by equation (15).

$$\begin{cases} P_0 = (h_v + J_{Q\min}) + \int_0^{\tau_{end}} (v_A - v_{B1}(\tau)) d\tau \\ P_0 = (h_v + J_{Q\min}) + \int_0^{\tau_0} (v_A - v_{B1}(\tau)) d\tau \\ P_0 = (h_v + J_{Q\min}) + \int_0^{\tau_0} (v_A - v_{B1}(\tau)) d\tau + \\ (v_A - v_{B1}(\tau_{Bend}))(\tau_{Cend} - \tau_{Bend}) \end{cases} \quad (15)$$

In equation (15), when  $\tau_{Bend}$  is greater than  $\tau_{Cend}$ , the first line of equation can be converted to the second line of equation. When  $\tau_{Bend}$  is less than  $\tau_{Cend}$ , the first equation can be converted to the third equation. The pseudo code for selecting the optimal strategy for multi-vehicle collaborative lane changing is as follows:

for Fleet B and C

    Divide fleet B and C into  $m/2$  units;

Vehicle number  $j$

$j=1$

    Enter the initial positions of vehicle  $C_{j+1}$  and  $B_{j+1}$

    for

$j \neq 1$

        if the initial position of vehicle  $C_{j+1}$  is greater than that of vehicle  $B_{j+1}$

            Implementation Strategy 1

        if the initial position of vehicle  $C_{j+1}$  is equal to the initial position of vehicle  $B_{j+1}$

            Implementation Strategy 2

        if the initial position of vehicle  $C_{j+1}$  is smaller than the initial position of vehicle  $B_{j+1}$

            Combining Implementation Strategy 1 and Strategy 2

    Fleet C

        Determine the spatial adjustment plan for fleet C

Vehicle number  $j$

$j=j+1$

end for  
 $j > n/2$   
 while not stop  
     for  $j \leq n/2$   
         Re-input the initial positions of vehicle  $C_{j+1}$  and vehicle  $B_{j+1}$

**IV. PERFORMANCE ANALYSIS AND EXPERIMENTAL VERIFICATION OF IAWM METHOD**

Simulation analysis was conducted to verify the effectiveness of IAWM. Therefore, this section mainly elaborates on the optimization of col-laborative lane changing strategies, model simulation verification, and overall simulation analysis and simulation comparison of IAWM.

**A. ANALYSIS OF PRIORITY SELECTION FOR COL-LABORATIVE LANE CHANGING STRATEGIES**

The first step was to optimize the multi-vehicle system lane changing strategy it utilized before verifying the effectiveness of IAWM. This process used a matrix laboratory to design the simulation program and used simulation to obtain the actual col-laborative lane changing time, speed, and ac-celeration parameters in the fleet unit. The optimal lane changing strategy for different initial relative positions was determined based on the actual simulation results. In the simulation process,  $J_{AB0}$  was set to 50m, and  $J_{AC0}$  was 49m.  $v_{B0}$ ,  $v'_{B0}$ ,  $v_{C0}$ , and  $v'_{C0}$  were 50 km/h.  $v_{A0}$  was 60 km/h,  $J_{Qmin}$  was 10m, and  $h_v$  was 5m. The ac-celeration values were between -2 m/s<sup>2</sup> and 2 m/s<sup>2</sup>, and  $v_{max}$  was 60 km/h. The initial relative distance between vehicle  $B_i$  and vehicle  $B_{j+1}$  in front was 15m and 20m. Vehicle  $C_{j+1}$  had 7 initial relative positions, namely parallel to vehicle  $B_{j+1}$ , 1m in front or behind vehicle  $B_{j+1}$ , 3m in front or behind vehicle  $B_{j+1}$ , and 5m in front or behind vehicle  $B_{j+1}$ . The study only conducted experiments on the set vehicle behavior, assuming that the initial speed of the vehicle is divided into two situations: 50km/h and 60km/h. In the actual driving process of the vehicle, the operating speed of the vehicle is within the range of 30km/h to 60km/h, and it can be seen that the parameters set in the study are reasonable and can be applied to practical scenarios. Under this parameter and constraint setting, the actual lane changing efficiency of vehicles  $C_{j+1}$  and  $B_{j+1}$  at 10 initial positions under two lane changing strategies was represented by 1-10. This process used the actual completed city of changing lanes as the evaluation indicator and represented the parameters  $J_{AC}$ ,  $J_{AB}$ ,  $J'_{AB}$ ,  $J'_{AB}$ ,  $\tau_v$ , and  $\tau_{end}$  as A~F. Table 1 shows the comparison results of lane changing efficiency at initial positions 1-4.

From Table 1, the difference in initial positions 1, 2, 3, and 4 was only due to the spatial distance between vehicle  $C_j$  and EV. The values of these two strategies at initial position 1 were equal, and the final lane change completion time was 13.31s. The final lane change completion time of strategy 1 under initial positions 2, 3, and 4 was lower than strategy 2, which was 13.31s. Figure 6 shows the comparison results of lane changing efficiency at initial positions 5-10.

**TABLE 1. Comparison results of lane changing efficiency at initial positions 1-4.**

		B <sub>j+1</sub> is 20m ahead of B <sub>i</sub> , C <sub>j+1</sub> is parallel to B <sub>i+1</sub>					
-		A	B	C	D	E	F
Strategy 1 (1)		49.00m	50.00m	70.00m	70.00m	7.72s	13.31s
Strategy 2 (1)		49.00m	50.00m	70.00m	70.00m	7.72s	13.31s
		B <sub>j+1</sub> is 20m ahead of B <sub>j</sub> , C <sub>j+1</sub> is 20m ahead of B <sub>j+1</sub>					
-		A	B	C	D	E	F
Strategy 1 (2)		49.00m	50.00m	71.00m	70.00m	7.72s	13.31s
Strategy 2 (2)		49.00m	50.00m	71.00m	70.00m	7.54s	13.5s
Strategy 1 (3)		49.00m	50.00m	73.00m	70.00m	7.72s	13.31s
Strategy 2 (3)		49.00m	50.00m	73.00m	70.00m	7.18s	13.85s
Strategy 1 (4)		49.00m	50.00m	75.00m	70.00m	7.72s	13.31s
Strategy 2 (4)		49.00m	50.00m	75.00m	70.00m	6.82s	14.21s

In Figure 6, there is a premise that  $B_{j+1}$  is 20m ahead of  $B_j$  and  $C_{j+1}$  lags behind of  $B_{j+1}$  20m at initial positions 5-7. There is a premise that  $B_{j+1}$  is 5m ahead of  $B_j$  at the initial positions of 8-10. From Figure 6 (a), the final lane change completion time of strategy 2 at initial position 5 was 13.13s lower than strategy 1, and these two strategies have the same time at initial position 6. From Figure 6 (b), the time for strategy 1 at initial position 7 was 13.13s lower than strategy 2, and the time for these two strategies at initial position 8 was equal. From Figure 6 (c), the time for strategy 1 at initial position 9 was 12.41s lower than strategy 2, and the final lane change completion time for strategy 2 at initial position 10 was 12.23s lower than strategy 1. Based on Tables 1 and 4, the position of vehicle  $C_{j+1}$  relative to  $B_{j+1}$  under the strategy did not affect the values of parameters E and F. In strategy 2, when the initial position of vehicle  $B_{j+1}$  was fixed, the larger the actual initial distance between vehicles  $C_{j+1}$  and  $B_{j+1}$ , the smaller the parameter E and the larger the parameter F. When vehicles  $C_{j+1}$  and  $B_{j+1}$  were driving in parallel, the values of parameters E and F were equal under both strategies. When the actual initial distance between vehicles  $B_j$  and  $B_{j+1}$  decreased, the parameter E increased and the parameter F decreased.

Research began to analyze their actual operating characteristics after exploring the impact of initial relative distance on the actual lane changing process of vehicles under two strategies. Assuming that the actual spatial distance between  $B_{j+1}$  and EV was 70m, three initial relative distances were set:  $C_{j+1}$  was 5m ahead of  $B_{j+1}$ ,  $C_{j+1}$  was parallel to  $B_{j+1}$ , and  $C_{j+1}$  was 10m behind  $B_{j+1}$ , represented by G~I. Figure 7 shows the ac-celeration variation characteristics of vehicles under different initial relative distances.

From Figure 7 (a), under strategy 1, the ac-celeration variation of vehicle  $C_{j+1}$  ranged from -2 to 2 m/s<sup>2</sup>, and all reached their extreme values at 6s. From Figure 7 (b), the amplitude of change significantly decreased under strategy 2. The ac-celeration variation of vehicle  $B_{j+1}$  under strategy 2



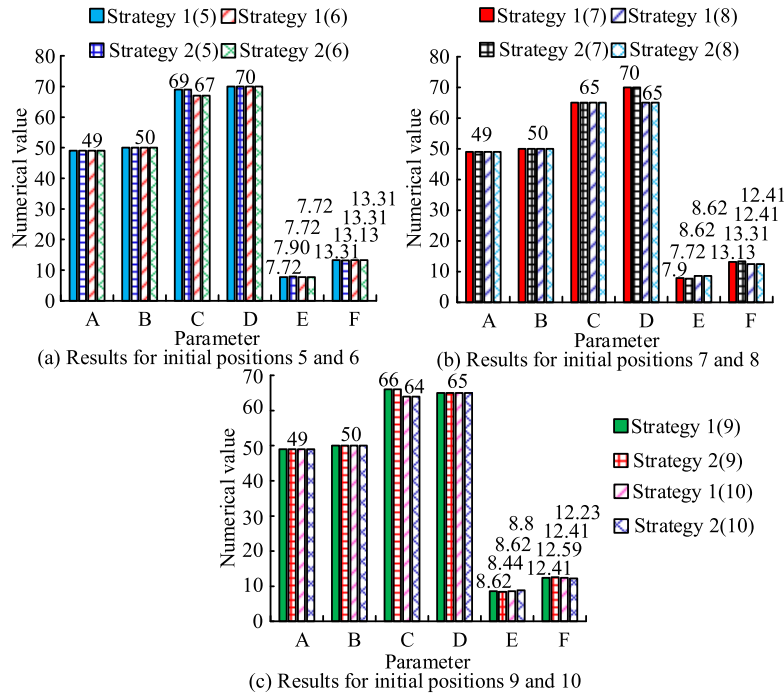


FIGURE 6. Comparison results of lane changing efficiency at initial positions 5-10.

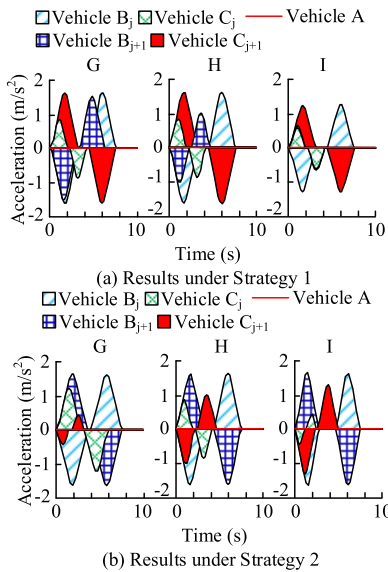


FIGURE 7. Result of ac-celeration variation characteristics of vehicles under different initial relative distances.

was between  $-2 \text{ m/s}^2$  and  $2 \text{ m/s}^2$ , and it also reached its extreme value at 6s, but the amplitude of variation under strategy 1 was significantly reduced. Overall, under strategy 2, the relative distance of initialization between vehicles  $C_{j+1}$  and  $B_{j+1}$  had a more significant impact on ac-celeration, and the actual adjustment methods of ac-celeration among these four vehicles were also different. Figure 8 shows the speed variation characteristics of vehicles under different initial relative distances.

From Figure 8 (a), the speed of vehicle  $C_{j+1}$  under strategy 1 showed a positive correlation with time at 0-5s,

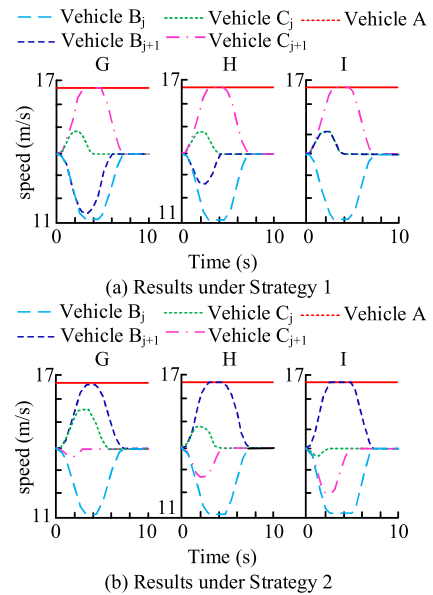


FIGURE 8. Result of speed variation characteristics of vehicles under different initial relative distances.

reaching an extreme value of  $16.85 \text{ m/s}$  around 4s, and a negative correlation after 5s. From Figure 8 (b), under strategy 2, its speed showed a negative correlation with time at 0-4s, and a parallel relationship after 4s. Based on Figures 8 and 6, when the initial relative positions of  $C_{j+1}$  and  $B_{j+1}$  were in a parallel state, the change process in strategies 1 and 2 was similar, that is, the speed and ac-celeration of car  $B_j$  and  $C_j$  both changed, and the adjustment order of  $C_{j+1}$  and  $B_{j+1}$  was different in different schemes. Therefore, the optimal strategy of MVCLC is the same as that in Figure 7, which

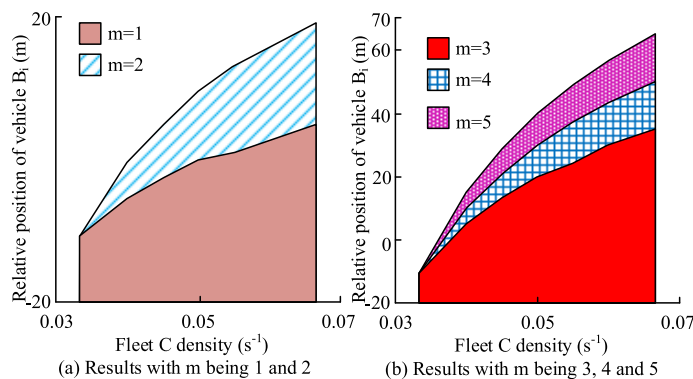


FIGURE 9. The relation-ship between the density of fleet C and the relative position of fleet B1.

has been effectively validated, indicating that the strategy is effective and scientific.

**B. MODEL SOLVING AND ANALYSIS**

On the basis of verifying the strategy, the study continued to simulate and analyze the constructed model to clarify the actual operating characteristics and variation patterns of vehicles during the process of the fleet only giving way. During this process, the initial speeds of fleets B and C were set to be 13.89 m/s, while the initial speed of EV A was 16.67 m/s. During the EV priority traffic control period, the maximum and minimum driving speeds of vehicles in fleet A and B were 16.67 m/s and 6.944 m/s, respectively. The actual vehicle length and the minimum safe distance between vehicles were 5m and 10m, respectively. The maximum ac-celerations of vehicles B1 and C1 were both  $\pm 2$  m/s<sup>2</sup>. Based on this, in the analysis of the fleet gap adjustment model, when the actual number of vehicles in fleet B is 1-5, Figure 9 shows the relative position of the density of fleet C and fleet B1.

From Figure 9 (a), when the number of fleet B was 1-2, the density of fleet C was directly proportional to the relative position of vehicle B1. From Figure 9 (b), when the number of fleet B was 3-5, the relation-ship between these two was also in contrast, but the growth rate was greater compared to (a). Overall, when the actual density of fleet C was about  $0.033m^{-1}$ , the relative displacement value of vehicle B1 was -10m, indicating that the distance between vehicles in fleet C could meet the conditions for vehicles in fleet B to directly merge. Therefore, the relative displacement of vehicle B1 as a whole depended on the initial longitudinal distance between B1 and C1. Mean-while, the number of vehicles had a significant impact on the relative position of vehicle B1. Under other traffic density conditions except for  $0.033m^{-1}$ , the relative displacement of B1 increased with the increase of the number of vehicles. Especially at a density of  $0.067m^{-1}$ , the number of vehicles in fleet B increased from 1 to 5. The longitudinal displacement of B1 increased from 5m to 65m, and the distance changed significantly. Therefore, based on the results of equation (9) and Figure 9, the initial ac-celeration value of B1 was set, and equation (13) was used to set the actual ac-celeration value of B1 in Table 2.

From Table 2, the initial ac-celeration value of vehicle B1 under the density change of fleet C was always  $-2, 0, \text{ or } 2$ . As the density of fleet C increased, the ac-celeration of vehicle B1 changed from positive to negative. When there were more than 3 vehicles in fleet B, the ac-celeration of B1 was positive only when the density of fleet C was  $+0.0333m^{-1}$ . At other traffic densities, the ac-celeration of B1 was negative. These results confirmed that after the control moment was activated, B1 slowed down before the speed trajectory adjustment was completed, with an ac-celeration of 0, and the car maintained a constant speed until EV exceeded. Especially when the traffic density of fleet C was relatively high, as the traffic density increased, the de-celeration of B1 also decreased due to the limitation of the minimum speed. Figure 10 shows the time for vehicle B1 to complete speed trajectory adjustment.

From Figure 10 (a), when the number of fleet B was 1, the time consumption of fleet C showed a trend of first decreasing and then increasing under the density change, with the lowest occurring at 0.04s. When it was 2, the lowest value appeared at 0.05. From Figure 10 (b), when the number of fleet B was 3-5, the time consumption of fleet C showed a continuous increasing trend under the density change. Overall, the maximum adjustment time for B1 reached 9.358s. When the number of vehicles  $\leq 2$  and the traffic density of fleet C was low, the adjustment time fluctuation of B1 was affected by its initial position, which was different from the fluctuation of the adjustment time. In the analysis of the fleet convergence model, after MVCLC control was activated, the actual ac-celeration of C1 was calculated using equation (11) in Table 3.

From Table 3, the speed was limited when there were many vehicles and the actual density of fleet C was high. Therefore, as the density of traffic and the number of fleet C increased, the de-celeration of C1 decreased. Its trend of change was basically consistent with B1. However, when the number of vehicles and traffic density were equal, the decrease in C1 compared to B1 was smaller. Similarly, the actual adjustment time of vehicle C1, the total dynamic trajectory adjustment time of these two fleets, and the minimum communication distance between EV and

TABLE 2. The initial ac-celeration value of B1 and the actual ac-celeration value setting result.

		Initial ac-celeration (m/s <sup>2</sup> )					
		$\kappa_C$					
m	+0.033	+0.040	+0.045	+0.050	+0.055	+0.060	+0.067
1	2.000			0.000	-2.000		
2	2.000	0	-2.000				
3							
4	2.000	-2.000					
5							
		Actual ac-celeration (m/s <sup>2</sup> )					
		$\kappa_C$					
m	+0.033	+0.040	+0.045	+0.050	+0.055	+0.060	+0.067
1	2.000	1.542	0.871	0.000	-2.000		
2	2.000	0.000	-2.000	-2.000			
3	2.000	-2.000			-1.894	-1.607	-1.377
4	2.000	-2.000		-1.607	-1.293	-1.112	-0.964
5	2.000	-2.000	-1.668	-1.205	-0.982	-0.850	-0.741

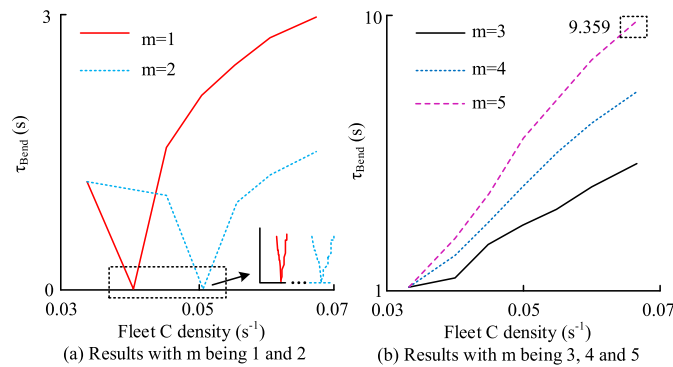


FIGURE 10. Time result of vehicle B1 completing speed trajectory adjustment.

TABLE 3. Actual ac-celeration result of C1.

		$\kappa_C$					
m	+0.033	+0.040	+0.045	+0.050	+0.055	+0.060	+0.067
1			2.000m/s <sup>2</sup>	0.000m/s <sup>2</sup>	-2.000m/s <sup>2</sup>	-2.000m/s <sup>2</sup>	-2.000m/s <sup>2</sup>
2		-2.000m/s <sup>2</sup>	-2.000m/s <sup>2</sup>	-2.000m/s <sup>2</sup>	-2.000m/s <sup>2</sup>	-1.808m/s <sup>2</sup>	-1.607m/s <sup>2</sup>
3	0.000m/s <sup>2</sup>			-1.607m/s <sup>2</sup>	-1.359m/s <sup>2</sup>	-1.205m/s <sup>2</sup>	-1.071m/s <sup>2</sup>
4			-1.549m/s <sup>2</sup>	-1.205m/s <sup>2</sup>	-1.018m/s <sup>2</sup>	-0.903m/s <sup>2</sup>	-0.803m/s <sup>2</sup>
5		-1.928m/s <sup>2</sup>	-1.238m/s <sup>2</sup>	-0.964m/s <sup>2</sup>	-0.815m/s <sup>2</sup>	-0.722m/s <sup>2</sup>	-0.642m/s <sup>2</sup>

B1 were calculated using equations (11), (14), and (15) in Figure 11.

From Figure 11 (a), except for the density of fleet C which was +0.0333m<sup>-1</sup>, the actual adjustment time of vehicle C1 at all other densities was gradually increasing. That is, the number of fleet B was proportional to the change in traffic density of fleet C. Compared with Figures 9 and 10, C1 completed the speed trajectory adjustment more slowly than B1. The maximum adjustment time for B1 was 9.358s, and the maximum adjustment time for C1 was 10.798s. The reason is that when the speed tracks of both parties are adjusted, C1 is arranged after B1, so the longitudinal relative displacement of vehicle C1 is greater than B1, and C1 needs more time to complete the speed trajectory adjustment. From Figure 11 (b), the total time for adjusting the dynamic trajectory of both fleets continuously increased with the density of fleet C,

which was influenced by the density of fleet C and the number of fleet B. From Figure 11 (c), as the number of vehicles in fleet B and the density of vehicles in fleet C increased, the minimum communication distance also increased. When the density of fleet C was 0.0667m<sup>-1</sup>, the number of vehicles in fleet B increased from 1 to 5, and the minimum communication distance increased from 31.26s to 119.992s. That is to say, for every additional vehicle in the fleet, the minimum communication distance needs to be increased by 20s.

C. IAWM SIMULATION ANALYSIS AND COMPARISON

The study began to simulate and verify the effectiveness of the proposed IAWM control method based on the optimal control strategy and model simulation analysis. Before the experiment, the vehicle type and parameters were set in Table 4.

TABLE 4. Vehicle types and parameters for simulation experiments.

-	1 (m)	2 (m)	3 (m)	4 (m/s)	5 (m/s <sup>2</sup> )	6 (m/s <sup>2</sup> )	7 (m/s <sup>2</sup> )	8
Social vehicles	4.0	1.8	2.0	20.0	3.0	4.4	9.0	IDM
Emergency vehicles	7.0	2.2	2.5	25.0	2.4	3.4	7.0	IDM
-	9	10	11	12	13	14	15	
Social vehicles	SL2015				1.1	0.1		
Emergency vehicles	SL2015	1.0	0.5	1.0	1.4	0.2	Arbitrarily	-

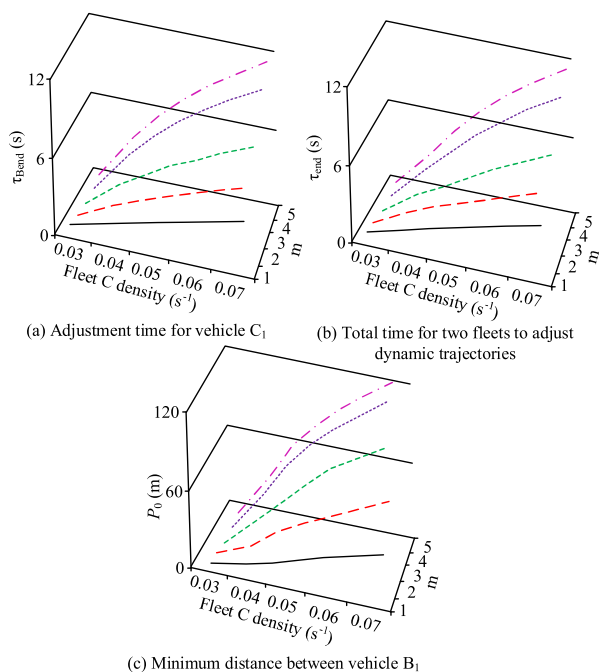


FIGURE 11. Vehicle C1 adjustment time, total dynamic trajectory adjustment time of two fleets, and minimum communication distance between emergency vehicles and B1 results.

In Table 4, 1-15 represent the length, width, minimum spacing, maximum speed, ac-celeration, de-celeration, maximum de-celeration, following and lane changing model, driver’s minimum reaction time, minimum lateral gap and maximum lateral speed, speed factor, speed factor deviation, and lateral arrangement of the vehicle, respectively. From Table 4, the EV ac-celeration and de-celeration were 2.4 m/s<sup>2</sup> and 3.4 m/s<sup>2</sup>, respectively, which were lower than the 3.0 m/s<sup>2</sup> and 4.4 m/s<sup>2</sup> of social vehicles. Both types of vehicles chose the Intelligent Driver Model (IDM) for their following model and the Set Lane Change Mode 2015 (SL2015) for lane changing model. Figure 12 shows the spatio-temporal distribution of EVs under IAWM control and the comparison of average driving speeds between EVs and social vehicles.

In Figure 12, pcu represents Passenger Car Unit (PCU), E is EV, and O is social vehicle. From Figure 12 (a), the operating trajectories of EVs were similar under four different traffic volumes, and the total travel time increased with the increase of traffic volume. Its EV driving time at 2000 pcu/h, 2500 pcu/h, and 3000 pcu/h increased by 1.69%, 5.52%, and 8.72% compared to the actual driving time at 1400 pcu/h.

TABLE 5. Comparison of results from different methods.

Method	Average driving speed (m/s)	Lane change completion time (s)
IAWM	24.16	13.08
T	20.35	20.42
Y	22.23	16.73

From Figure 12 (b), when the actual communication distance exceeded 45m at 1400 pcu/h, the driving speed of the EV was still relatively stable, but the driving speed of social vehicles was significantly reduced. The communication distance exceeding 75s at 3000 pcu/h was also the same, which was consistent with the calculation result of the three-line formula in equation (15), proving the high accuracy of IAWM. The study introduced the traditional yield Model (T) and lane selection Model (Y), and compared the driving speeds of EV and social vehicles under the control of these three models to further verify the superiority of IAWM [32], [33]. Figure 13 shows the results.

From Figure 13, IAWM significantly improved the driving speed of EVs in various traffic streams. Compared with Model T, it increased by 6.34% at 1400 pcu/hour. At 2500 pcu/hour, its driving speed increased by 6.05%, and the average speed increased by 12.64% under four different flow conditions. Compared with Model Y, the IAWM controlled EV at 1400 pcu/h reduced driving speed by 1.85%. When the traffic volume increased, the speed of both control methods decreased in emergency situations. At a vehicle flow rate of 3000 pcu/hour, the vehicle operating speed controlled by IAWM was 7.34% faster than that controlled by BLM. In addition, compared with Model Y, the average flow rate of IAWM decreased by 1.45% under four experimental flow rates. At 1400 pcu/h, its speed increased by 1.27%. After the traffic flow increased to 2500 pcu/h, its speed decreased by 2.90%. Overall, IAWM focuses more on using IoV technology support to achieve col-laborative lane changing between social vehicles and EVs, with the fleet as the research object. It enables the fleet of social vehicles to merge into adjacent lanes in a shorter period of time, thereby achieving rapid movement of EVs. The research method was applied to practical scenarios, the traffic volume was set to 2000pcu/h, and the average driving speed and lane change completion time of EVs were analyzed under different methods, as shown in Table 5.

From Table 5, the research method had a faster average driving speed and faster lane completion time compared to the other two methods. Among them, the average driving speed

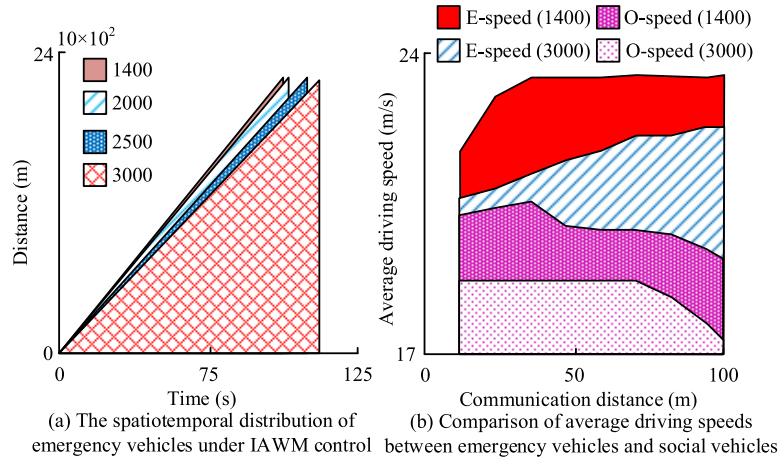


**FIGURE 12. The spatiotemporal distribution of emergency vehicles under IAWM control and the comparison of average driving speeds between emergency vehicles and social vehicles.**

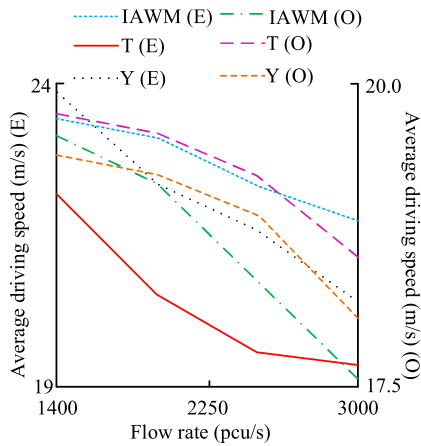


**FIGURE 13. Comparison of the driving speeds of emergency vehicles and social vehicles under the control of three models.**

of the IAWM method was 24.16m/s, which was 3.81m/s higher than Model T and 1.93m/s higher than Model Y. As a result, the research method had good performance and effectively solved the problem of EVs changing lanes quickly.

**V. CONCLUSION**

The current EV priority traffic control method in the road traffic net-work is difficult to cope with the increasing traffic demand environment. In this regard, the study proposed an IAWM control model for road traffic net-works in emergency situations and verified its effectiveness. These experiments confirmed that under strategy 2, when the initial position of vehicle B<sub>j+1</sub> was fixed, the larger the actual initial distance between vehicles C<sub>j+1</sub> and B<sub>j+1</sub>, the smaller the parameter E and the larger the parameter F. Under strategy 2, its speed showed a negative correlation with time between 0 and 4s, and a parallel relation-ship after 4s. In addition, when the actual density of fleet C was about 0.033m<sup>-1</sup>, the relative dis-placement value of vehicle B1 was -10m, indicating that the distance between vehicles in fleet C met the conditions for vehicles in fleet B to directly merge.

The maximum time for B1 regulation was 9.358s, and the maximum time for C1 regulation was 10.798s. Mean-while, the driving time of EVs at 2000 pcu/h, 2500 pcu/h, and 3000 pcu/h increased by 1.69%, 5.52%, and 8.72% compared to 1400 pcu/h. Compared with Model T, it increased by 6.34% at 1400 pcu/hour. Compared with Model Y, the IAWM controlled EV at 1400 pcu/h reduced driving speed by 1.85%. Overall, the IAWM proposed based on the Duce col-laborative lane changing strategy and these two models constructed using IoV is feasible and effective. However, in the analysis of the priority selection problem for EV road sections, only a scenario of one-way two lanes is constructed. Subsequent analysis of bilateral lane changing under multi-lane conditions is needed to improve the applicability of IAWM.

**REFERENCES**

- [1] M. Hasanvand, "Machine learning methodology for identifying vehicles using image processing," *Artif. Intell. Appl.*, vol. 1, no. 3, pp. 170–178, Jul. 2023, doi: 10.47852/bonviewaia3202833.
- [2] W. Hu, X. Li, J. Hu, X. Song, X. Dong, D. Kong, Q. Xu, and C. Ren, "A rear anti-collision decision-making methodology based on deep reinforcement learning for autonomous commercial vehicles," *IEEE Sensors J.*, vol. 22, no. 16, pp. 16370–16380, Aug. 2022, doi: 10.1109/JSEN.2022.3190302.
- [3] J. Peng, S. Zhang, Y. Zhou, and Z. Li, "An integrated model for autonomous speed and lane change decision-making based on deep reinforcement learning," *IEEE Trans. Intell. Transp. Syst.*, vol. 23, no. 11, pp. 21848–21860, Nov. 2022, doi: 10.1109/TITS.2022.3185255.
- [4] A. K. Erenoglu and O. Erdinc, "Real-time allocation of multi-mobile resources in integrated distribution and transportation systems for resilient electrical grid," *IEEE Trans. Power Del.*, vol. 38, no. 2, pp. 1108–1119, Apr. 2023, doi: 10.1109/TPWRD.2022.3206272.
- [5] P. Choudhary and R. K. Dwivedi, "A novel algorithm for traffic control using thread based virtual traffic light," *Int. J. Inf. Technol.*, vol. 14, no. 1, pp. 115–124, Feb. 2022, doi: 10.1007/s41870-021-00808-6.
- [6] Y. Wu, F. Pan, S. Li, Z. Chen, and M. Dong, "Peer-induced fairness capacitated vehicle routing scheduling using a hybrid optimization ACO-VNS algorithm," *Soft Comput.*, vol. 24, no. 3, pp. 2201–2213, Feb. 2020, doi: 10.1007/s00500-019-04053-9.
- [7] D. Das, N. V. Altekar, K. L. Head, and F. Saleem, "Traffic signal priority control strategy for connected emergency vehicles with dilemma zone protection for freight vehicles," *Transp. Res. Rec.*, vol. 2676, no. 1, pp. 499–517, Aug. 2022, doi: 10.1177/03611981211039157.

- [8] M. Miletic, E. Ivanjko, M. Greguric, and K. Kušic, "A review of reinforcement learning applications in adaptive traffic signal control," *IET Intell. Transp. Syst.*, vol. 16, no. 10, pp. 1269–1285, Jun. 2022, doi: 10.1049/itr2.12208.
- [9] A. A. Monisha, T. R. Reshmi, and K. Murugan, "Secure relay selection scheme for traffic congested zone in VANET using grasshopper optimization and modified authentication key agreement algorithms," *Appl. Intell.*, vol. 53, no. 5, pp. 497–5518, Mar. 2023, doi: 10.1007/s10489-022-03572-7.
- [10] R. Nakahara, K. Sekiguchi, K. Nonaka, M. Takasugi, H. Hasebe, and K. Matsubara, "Stochastic model predictive braking control for heavy-duty commercial vehicles during uncertain brake pressure and road profile conditions," *Control Theory Technol.*, vol. 20, no. 2, pp. 248–262, May 2022, doi: 10.1007/s11768-022-00090-2.
- [11] M. B. Younes and A. Boukerche, "Safety and efficiency control protocol for highways using intelligent vehicular networks," *Comput. Netw.*, vol. 152, pp. 1–11, Apr. 2019, doi: 10.1016/j.comnet.2019.01.016.
- [12] Z. Wang, X. Zhao, Z. Xu, X. Li, and X. Qu, "Modeling and field experiments on autonomous vehicle lane changing with surrounding human-driven vehicles," *Computer-Aided Civil Infrastructure Eng.*, vol. 36, no. 7, pp. 877–889, Jul. 2021, doi: 10.1111/mice.12540.
- [13] S. Hussain, Y.-S. Kim, S. Thakur, and J. G. Breslin, "Optimization of waiting time for electric vehicles using a fuzzy inference system," *IEEE Trans. Intell. Transp. Syst.*, vol. 23, no. 9, pp. 15396–15407, Sep. 2022, doi: 10.1109/TITS.2022.3140461.
- [14] Q. Wei and C. Zhou, "A multi-criteria decision-making framework for electric vehicle supplier selection of government agencies and public bodies in China," *Environ. Sci. Pollut. Res.*, vol. 30, no. 4, pp. 10540–10559, Sep. 2022, doi: 10.1007/s11356-022-22783-6.
- [15] Z. Liu, H. Jia, R. Wu, J. Tian, and G. Wang, "IoV-based mathematic model for platoon give way to emergency vehicles promptly," *IEEE Trans. Intell. Transp. Syst.*, vol. 23, no. 9, pp. 16280–16289, Sep. 2022, doi: 10.1109/TITS.2022.3149519.
- [16] M. Cao, V. O. K. Li, and Q. Shuai, "A gain with no pain: Exploring intelligent traffic signal control for emergency vehicles," *IEEE Trans. Intell. Transp. Syst.*, vol. 23, no. 10, pp. 17899–17909, Oct. 2022, doi: 10.1109/TITS.2022.3159714.
- [17] M. Hosseinzadeh, B. Sinopoli, I. Kolmanovsky, and S. Baruah, "MPC-based emergency vehicle-centered multi-intersection traffic control," *IEEE Trans. Control Syst. Technol.*, vol. 31, no. 1, pp. 166–178, Jan. 2023, doi: 10.1109/TCST.2022.3168610.
- [18] A. A. A. Alkhatib, K. A. Maria, S. AlZu'bi, and E. A. Maria, "Smart traffic scheduling for crowded cities road networks," *Egyptian Informat. J.*, vol. 23, no. 4, pp. 163–176, Dec. 2022, doi: 10.1016/j.eij.2022.10.002.
- [19] G. Raja and G. Saravanan, "Eco-friendly disaster evacuation framework for 6G connected and autonomous vehicular networks," *IEEE Trans. Green Commun. Netw.*, vol. 6, no. 3, pp. 1368–1376, Sep. 2022, doi: 10.1109/TGCN.2022.3163764.
- [20] G.-P. Antonio and C. Maria-Dolores, "Multi-agent deep reinforcement learning to manage connected autonomous vehicles at tomorrow's intersections," *IEEE Trans. Veh. Technol.*, vol. 71, no. 7, pp. 7033–7043, Jul. 2022, doi: 10.1109/TVT.2022.3169907.
- [21] D. Jutury, N. Kumar, A. Sachan, Y. Daultani, and N. Dhakad, "Adaptive neuro-fuzzy enabled multi-mode traffic light control system for urban transport network," *Appl. Intell.*, vol. 53, no. 6, pp. 7132–7153, Mar. 2023, doi: 10.1007/s10489-022-03827-3.
- [22] R. Hajiloo, A. Khajepour, A. Kasaiezadeh, S.-K. Chen, and B. Litkouhi, "Integrated lateral and roll stability control of multi-actuated vehicles using prioritization model predictive control," *IEEE Trans. Veh. Technol.*, vol. 71, no. 8, pp. 8318–8329, Aug. 2022, doi: 10.1109/TVT.2022.3174172.
- [23] M. Cai, Q. Xu, C. Chen, J. Wang, K. Li, J. Wang, and Q. Zhu, "Formation control for connected and automated vehicles on multi-lane roads: Relative motion planning and conflict resolution," *IET Intell. Transp. Syst.*, vol. 17, no. 1, pp. 211–226, Jul. 2022, doi: 10.1049/itr2.12249.
- [24] M. Ramya Devi, I. Jasmine Selvakumari Jeya, and S. Lokesh, "Adaptive scheduled partitioning technique for reliable emergency message broadcasting in VANET for intelligent transportation systems," *Automatika*, vol. 64, no. 2, pp. 341–354, Nov. 2022, doi: 10.1080/00051144.2022.2140392.
- [25] Z. Li, H. Chen, H. Liu, P. Wang, and X. Gong, "Integrated longitudinal and lateral vehicle stability control for extreme conditions with safety dynamic requirements analysis," *IEEE Trans. Intell. Transp. Syst.*, vol. 23, no. 10, pp. 19285–19298, Oct. 2022, doi: 10.1109/TITS.2022.3152485.
- [26] X. Cao, L. Jin, F. Huang, Z. Liu, and R. Xiu, "Application of smart grid communication service flow modeling based on Poisson model in grid operation," *J. Cases Inf. Technol.*, vol. 24, no. 5, pp. 1–12, Jun. 2022, doi: 10.4018/jcit.302243.
- [27] R. Lloret-Battle, Z.-H. Wang, and J. Zheng, "Traffic volume estimation for both undersaturated and oversaturated signalized intersections with stopbar location estimation using trajectory data," *Transp. Res. Record: J. Transp. Res. Board.*, vol. 2677, no. 3, pp. 343–354, Mar. 2023, doi: 10.1177/03611981221115073.
- [28] M. Klischat and M. Althoff, "Falsifying motion plans of autonomous vehicles with abstractly specified traffic scenarios," *IEEE Trans. Intell. Vehicles*, vol. 8, no. 2, pp. 1717–1730, Feb. 2023, doi: 10.1109/TIV.2022.3191179.
- [29] L. Wang, M. Yang, Y. Li, B. Wang, and J. Zhang, "Resolution strategies for cooperative vehicle fleets for reducing rear-end collision risks near recurrent freeway bottlenecks," *J. Intell. Transp. Syst.*, vol. 27, no. 5, pp. 587–605, Sep. 2023, doi: 10.1080/15472450.2022.2070432.
- [30] C. Vishnu, V. Abhinav, D. Roy, C. K. Mohan, and Ch. S. Babu, "Improving multi-agent trajectory prediction using traffic states on interactive driving scenarios," *IEEE Robot. Autom. Lett.*, vol. 8, no. 5, pp. 2708–2715, May 2023, doi: 10.1109/LRA.2023.3258685.
- [31] B. Feng, Y. Huang, A. Tian, H. Wang, H. Zhou, S. Yu, and H. Zhang, "DR-SDSN: An elastic differentiated routing framework for software-defined satellite networks," *IEEE Wireless Commun.*, vol. 29, no. 6, pp. 80–86, Dec. 2022, doi: 10.1109/MWC.011.2100578.
- [32] X. Kong, G. Duan, M. Hou, G. Shen, H. Wang, X. Yan, and M. Collotta, "Deep reinforcement learning-based energy-efficient edge computing for Internet of Vehicles," *IEEE Trans. Ind. Informat.*, vol. 18, no. 9, pp. 6308–6316, Sep. 2022, doi: 10.1109/TII.2022.3155162.
- [33] X. He, H. Yang, Z. Hu, and C. Lv, "Robust lane change decision making for autonomous vehicles: An observation adversarial reinforcement learning approach," *IEEE Trans. Intell. Vehicles*, vol. 8, no. 1, pp. 184–193, Jan. 2023, doi: 10.1109/TIV.2022.3165178.



**XILIANG WANG** was born in Pingdu, in December 1966. He received the bachelor's and master's degrees in geological engineering from China University of Mining and Technology, in 1989 and 1993, respectively, and the Ph.D. degree in engineering geology from China University of Mining and Technology (Beijing), in July 2000.

From 1989 to 1997, he was an Engineer with Xingtai Mining Technology Department, Xingtai Mining Bureau. Since 2000, he has been a Professor with the School of Transportation, Shijiazhuang Tiedao University. He has coauthored some papers, including the Vulnerability analysis of subway systems based on complex network models and the Analysis of tourism traffic behavior in Beijing-Tianjin-Hebei region based on structural equation model and the book *Light Environment Control of Expressway Tunnels* (Science Press, 2021). He has hosted the key project: Hebei Provincial Department of Science and Technology: Research on Safety Prevention and Control and Rapid Accident Repair Technology for Expressway Tunnel Operation, in 2021.



**HUIJIAN GENG** was born in Gaocheng, Hebei, in January 1980. He received the bachelor's degree in economic information management from Hebei University of Economics and Business, in 2002, the master's degree in testing and metrology technology and instruments from Hebei University of Science and Technology, in 2008, and the Ph.D. degree in transportation and management from Shijiazhuang Tiedao University. He is currently a Senior Political Engineer. He has led and participated in more than 20 provincial-level projects, published nearly 20 articles, and two monographs. His research interest includes transportation management.

•••